

CHAPTER 4 NUMERICAL RESULTS

This chapter is to verify the numerical solutions of the generalized Burgers–Huxley equation, and to test the efficiency and viability of the proposed methods (method $M_1(\theta)$ and method $M_2(\theta)$). The following generalized Burgers–Huxley equation problem is considered:

$$\frac{\partial u}{\partial t} + \alpha u^\delta \frac{\partial u}{\partial x} - \frac{\partial^2 u}{\partial x^2} = \beta u(1 - u^\delta)(u^\delta - \gamma), \quad 0 \leq x \leq 1, t \geq 0 \quad (4.1)$$

with the initial condition

$$u(x, 0) = \left(\frac{\gamma}{2} + \frac{\gamma}{2} \tanh(\mu x) \right)^{1/\delta} \quad (4.2)$$

and the boundary condition:

$$u(0, t) = \left(\frac{\gamma}{2} + \frac{\gamma}{2} \tanh(-\mu ct) \right)^{1/\delta}, \quad t \geq 0, \quad (4.3)$$

$$u(L, t) = \left(\frac{\gamma}{2} + \frac{\gamma}{2} \tanh[\mu(L - ct)] \right)^{1/\delta}, \quad t \geq 0. \quad (4.4)$$

From chapter 3 section 3.1, it is found that, under the initial and boundary conditions (4.2)-(4.4), the exact solution of (4.1)-(4.4) is given by

$$u(x, t) = \left(\frac{\gamma}{2} + \frac{\gamma}{2} \tanh[\mu(x - ct)] \right)^{1/\delta}, \quad (4.5)$$

where

$$\mu = \frac{\delta \gamma \left(\sqrt{\alpha^2 + 4\beta(\delta + 1)} - \alpha \right)}{4(\delta + 1)}, \quad (4.6)$$

$$c = \frac{\left(\alpha - \sqrt{\alpha^2 + 4\beta(\delta + 1)} \right) \gamma + \left(\alpha + \sqrt{\alpha^2 + 4\beta(\delta + 1)} \right) (\delta + 1)}{2(\delta + 1)}. \quad (4.7)$$

To verify the efficiency and to measure the accuracy of the methods $M_1(\theta)$ and $M_2(\theta)$ for the problem (4.1)-(4.4) in which compare with the exact solution (4.5)-(4.7), the numerical solution will be calculated using methods $M_1(\theta)$ and $M_2(\theta)$ for x in the interval $0 \leq x \leq 1$ at time $t = 10$ with $\theta = 1$, $\ell = 0.01$, $h = 0.1$ and vary the parameters α , β , γ and δ . The boundedness of the solution and the build-up for error may be examined with the relative error and two norms. The relative error is given by

$$\frac{|u(x_m, t_n) - U(x_m, t_n)|}{u(x_m, t_n)} \times 100, \quad (4.8)$$

where $u(x_m, t_n)$ and $U(x_m, t_n)$ denote the exact solution and the numerical solution at the mesh point (x_m, t_n) , $m = 0, 1, \dots, M$, $n = 0, 1, \dots, N$, respectively. Let $Z_m^n = u(x_m, t_n) - U(x_m, t_n)$ with $m = 0, 1, \dots, M$ and $n = 0, 1, \dots, N$ so that \mathbf{Z}^n is the vector of such errors and has $N + 1$ elements. The L_2 norm and L_∞ norm are given by

$$\|\mathbf{Z}^n\|_2 = \left(h \sum_{m=0}^M |Z_m^n|^2 \right)^{\frac{1}{2}} \quad (4.9)$$

and

$$\|\mathbf{Z}^n\|_\infty = \max_m |Z_m^n|, \quad (4.10)$$

respectively.

Firstly, the relative errors for various values of α , β , γ , and δ , at time $t = 10$, are tabulated in Tables 4.1-4.4. The sample data of all experiments are chosen at $x = 0.1, 0.5$ and 0.9 . It is seen that the relative errors of both methods $M_1(\theta)$ and $M_2(\theta)$ increase as the values α , β , γ and δ increase. Moreover, the relative errors of method $M_1(\theta)$ is lesser than method $M_2(\theta)$ for given parameters as shown in Tables 4.1-4.4.

Next, The L_2 and L_∞ norms produced by methods $M_1(\theta)$ and $M_2(\theta)$ at $t = 10$ for various values of α , β , γ , and δ are tabulated in Table 4.5. The results are similar to the relative errors. It is obvious that as parameters α , β , γ and δ increase the L_2 and L_∞ norms of both two methods also increase. Moreover, the L_2 and L_∞ norms of method $M_1(\theta)$ are lesser than method $M_2(\theta)$.

Table 4.1: The relative errors of the methods $M_1(\theta)$ and $M_2(\theta)$ at time $t = 10$ with $\alpha = 1$, $\beta = 1$, $\gamma = 0.001$, $\theta = 1$, $\ell = 0.01$, $h = 0.1$ and vary δ

α	β	γ	δ	x	Relative Errors	
					$M_1(\theta)$	$M_2(\theta)$
1	1	0.001	1	0.1	5.199674×10^{-11}	2.255828×10^{-8}
				0.5	1.433362×10^{-10}	6.266096×10^{-8}
				0.9	5.133265×10^{-11}	2.255750×10^{-8}
1	1	0.001	2	0.1	5.517687×10^{-9}	2.824004×10^{-8}
				0.5	1.532942×10^{-8}	7.844400×10^{-8}
				0.9	5.519026×10^{-9}	2.823919×10^{-8}
1	1	0.001	4	0.1	1.665152×10^{-8}	3.959749×10^{-8}
				0.5	4.626037×10^{-8}	1.099942×10^{-7}
				0.9	1.665442×10^{-8}	3.959685×10^{-8}

Table 4.2: The relative errors of the methods $M_1(\theta)$ and $M_2(\theta)$ at time $t = 10$ with $\alpha = 1$, $\beta = 1$, $\delta = 1$, $\theta = 1$, $\ell = 0.01$, $h = 0.1$ and vary γ

α	β	γ	δ	x	Relative Errors	
					$M_1(\theta)$	$M_2(\theta)$
1	1	0.01	1	0.1	5.394476×10^{-8}	2.305715×10^{-6}
				0.5	1.484872×10^{-7}	6.403631×10^{-6}
				0.9	5.312234×10^{-8}	2.304744×10^{-6}
1	1	0.5	1	0.1	5.570592×10^{-3}	4.774102×10^{-3}
				0.5	1.446046×10^{-2}	1.243465×10^{-2}
				0.9	4.877437×10^{-3}	4.204436×10^{-3}
1	1	0.9	1	0.1	1.903742×10^{-2}	1.243252×10^{-2}
				0.5	4.676584×10^{-2}	3.056215×10^{-2}
				0.9	1.499772×10^{-2}	9.805347×10^{-3}

Table 4.3: The relative errors of the methods $M_1(\theta)$ and $M_2(\theta)$ at time $t = 10$ with $\alpha = 1$, $\gamma = 0.01$, $\delta = 1$, $\theta = 1$, $\ell = 0.01$, $h = 0.1$ and vary β

α	β	γ	δ	x	Relative Errors	
					$M_1(\theta)$	$M_2(\theta)$
1	2	0.01	1	0.1	4.618936×10^{-7}	9.415083×10^{-6}
				0.5	1.272897×10^{-6}	2.613551×10^{-5}
				0.9	4.558941×10^{-7}	9.401198×10^{-6}
1	4	0.01	1	0.1	4.053694×10^{-6}	3.893077×10^{-5}
				0.5	1.117736×10^{-5}	1.079873×10^{-4}
				0.9	4.005061×10^{-6}	3.880922×10^{-5}
1	8	0.01	1	0.1	3.649480×10^{-5}	1.616383×10^{-4}
				0.5	1.000124×10^{-4}	4.478091×10^{-4}
				0.9	3.582234×10^{-5}	1.606952×10^{-4}

Table 4.4: The relative errors of the methods $M_1(\theta)$ and $M_2(\theta)$ at time $t = 10$ with $\beta = 1$, $\gamma = 0.01$, $\delta, \theta = 1$, $\ell = 0.01$, $h = 0.1$ and vary α

α	β	γ	δ	x	Relative Errors	
					$M_1(\theta)$	$M_2(\theta)$
2	1	0.01	1	0.1	5.575824×10^{-8}	2.305383×10^{-6}
				0.5	1.539506×10^{-7}	6.408218×10^{-6}
				0.9	5.524262×10^{-8}	2.308381×10^{-6}
4	1	0.01	1	0.1	5.711617×10^{-8}	2.303201×10^{-6}
				0.5	1.582761×10^{-8}	6.411795×10^{-6}
				0.9	5.699948×10^{-8}	2.313154×10^{-6}
8	1	0.01	1	0.1	5.767619×10^{-8}	2.297592×10^{-6}
				0.5	1.604984×10^{-7}	6.413501×10^{-6}
				0.9	5.804114×10^{-8}	2.320057×10^{-6}

Table 4.5: The L_2 and L_∞ norms for various values of α , β , γ , and δ at time $t = 10$ using the methods $M_1(\theta)$ and $M_2(\theta)$ with $\theta = 1$, $\ell = 0.01$ and $h = 0.1$

α	β	γ	δ	$\ Z^n\ _2$		$\ Z^n\ _\infty$	
				$M_1(\theta)$	$M_2(\theta)$	$M_1(\theta)$	$M_2(\theta)$
1	1	0.001	1	5.2096×10^{-16}	2.2768×10^{-13}	7.131×10^{-16}	3.1178×10^{-13}
1	1	0.001	2	2.4909×10^{-11}	1.2746×10^{-11}	3.4109×10^{-11}	1.7455×10^{-11}
1	1	0.001	4	5.0266×10^{-11}	1.1952×10^{-10}	6.8833×10^{-11}	1.6367×10^{-10}
1	1	0.01	1	5.1600×10^{-12}	2.2245×10^{-10}	7.0636×10^{-12}	3.0462×10^{-10}
1	1	0.5	1	7.4293×10^{-7}	6.3881×10^{-7}	1.0168×10^{-6}	8.7438×10^{-7}
1	1	0.9	1	3.6005×10^{-7}	2.3529×10^{-7}	4.9224×10^{-7}	3.2168×10^{-7}
1	2	0.01	1	4.1962×10^{-11}	8.6129×10^{-10}	5.7444×10^{-11}	1.1794×10^{-9}
1	4	0.01	1	3.2911×10^{-10}	3.1785×10^{-9}	4.5053×10^{-10}	4.3527×10^{-9}
1	8	0.01	1	2.2973×10^{-9}	1.0221×10^{-8}	3.1449×10^{-9}	1.3998×10^{-8}
2	1	0.01	1	5.3476×10^{-12}	2.2252×10^{-10}	7.3205×10^{-12}	3.0472×10^{-10}
4	1	0.01	1	5.4955×10^{-12}	2.2255×10^{-10}	7.5231×10^{-12}	3.0476×10^{-10}
8	1	0.01	1	5.5710×10^{-12}	2.2255×10^{-10}	7.6265×10^{-12}	3.0475×10^{-10}

It can be concluded that, from Tables 4.1-4.5, both methods are stable in the sense that all relative errors and error norms remain bounded.

The efficiency of methods $M_1(\theta)$ and $M_2(\theta)$ is monitored by comparing the numerical solutions of (4.1)-(4.4) produced by two methods with the exact solution (4.5). The simu-

lation results are shown in Figure 4.1. It is seen that, from Figure 4.1, the profiles of solution produced by two methods appear to be coincident with the exact solution. Clearly, the methods $M_1(\theta)$ and $M_2(\theta)$ give a reliable representation of the travelling waves associated with (4.1)-(4.4).

Table 4.6: The interval stabilities of methods $M_1(\theta)$ and $M_2(\theta)$ with $\alpha = 1$, $\beta = 1$, $\gamma = 0.001$ and $h = 0.1$ for various values of δ and θ : $\delta = 1, 2, 4$; $\theta = 0, \frac{1}{2}, 1$

α	β	γ	δ	θ	Interval of Stability	
					$M_1(\theta)$	$M_2(\theta)$
1	1	0.001	1	0	(0, 0.0051)	(0, 0.0051)
				$\frac{1}{2}$	(0, 14.3709)	(0, 11.2460)
				1	(0, 999.9999)	(0, ∞)
1	1	0.001	2	0	(0, 0.0051)	(0, 0.0051)
				$\frac{1}{2}$	(0, 9.5373)	(0, 9.5327)
				1	(0, 999.9999)	(0, ∞)
1	1	0.001	4	0	(0, 0.0051)	(0, 0.0051)
				$\frac{1}{2}$	(0, 4.7683)	(0, 4.7683)
				1	(0, 999.9999)	(0, ∞)

Table 4.7: The interval stabilities of methods $M_1(\theta)$ and $M_2(\theta)$ with $\alpha = 1$, $\beta = 1$, $\delta = 1$ and $h = 0.1$ for various values of γ and θ : $\gamma = 0.01, 0.5, 0.9$; $\theta = 0, \frac{1}{2}, 1$

α	β	γ	δ	θ	Interval of Stability	
					$M_1(\theta)$	$M_2(\theta)$
1	1	0.01	1	0	(0, 0.0051)	(0, 0.0051)
				$\frac{1}{2}$	(0, 1.8305)	(0, 1.6219)
				1	(0, 99.9999)	(0, ∞)
1	1	0.5	1	0	(0, 0.0051)	(0, 0.0051)
				$\frac{1}{2}$	(0, 0.0441)	(0, 0.0441)
				1	(0, 1.9999)	(0, ∞)
1	1	0.9	1	0	(0, 0.0051)	(0, 0.0051)
				$\frac{1}{2}$	(0, 0.0315)	(0, 0.0322)
				1	(0, 1.1111)	(0, ∞)

Table 4.8: The interval stabilities of methods $M_1(\theta)$ and $M_2(\theta)$ with $\alpha = 1$, $\gamma = 0.01$, $\delta = 1$ and $h = 0.1$ for various values of β and θ : $\beta = 2, 4, 8$; $\theta = 0, \frac{1}{2}, 1$

α	β	γ	δ	θ	Interval of Stability	
					$M_1(\theta)$	$M_2(\theta)$
1	2	0.01	1	0	(0, 0.0051)	(0, 0.0051)
				$\frac{1}{2}$	(0, 0.9564)	(0, 0.9564)
				1	(0, 49.9999)	(0, ∞)
1	4	0.01	1	0	(0, 0.0051)	(0, 0.0051)
				$\frac{1}{2}$	(0, 0.4784)	(0, 0.4784)
				1	(0, 24.9999)	(0, ∞)
1	8	0.01	1	0	(0, 0.0051)	(0, 0.0051)
				$\frac{1}{2}$	(0, 0.2394)	(0, 0.2394)
				1	(0, 12.4999)	(0, ∞)

Table 4.9: The interval stabilities of methods $M_1(\theta)$ and $M_2(\theta)$ with $\beta = 1$, $\gamma = 0.01$, $\delta = 1$ and $h = 0.1$ for various values of α and θ : $\alpha = 2, 4, 8$; $\theta = 0, \frac{1}{2}, 1$

α	β	γ	δ	θ	Interval of Stability	
					$M_1(\theta)$	$M_2(\theta)$
2	1	0.01	1	0	(0, 0.0051)	(0, 0.0051)
				$\frac{1}{2}$	(0, 1.8290)	(0, 1.6188)
				1	(0, 99.9999)	(0, ∞)
4	1	0.01	1	0	(0, 0.0051)	(0, 0.0051)
				$\frac{1}{2}$	(0, 1.8535)	(0, 1.6142)
				1	(0, 99.9999)	(0, ∞)
8	1	0.01	1	0	(0, 0.0051)	(0, 0.0051)
				$\frac{1}{2}$	(0, 1.8470)	(0, 1.6067)
				1	(0, 99.9999)	(0, ∞)

The effect of the time-step on the methods $M_1(\theta)$ and $M_2(\theta)$ with $\theta = 0, \frac{1}{2}, 1$ is monitored to evaluate the intervals of stability for the different values α , β , γ and δ . The stability intervals of numerical methods are tabulated in Tables 4.6-4.9. In the case method $M_1(\theta)$ with $\theta = 0$ produced overflow for $\ell > 0.0051$. Using $\theta = \frac{1}{2}$ and $\theta = 1$, method $M_1(\theta)$ produced overflow as ℓ increased above values in the stability intervals (see Tables 4.6-4.9). It is also verified that the stability intervals of method $M_1(\theta)$ depend on the parameters α , β , γ and δ . Using method $M_2(\theta)$ with $\theta = 0$, it is found that this method produced overflow for $\ell > 0.0051$. When $\theta = \frac{1}{2}$, method $M_2(\theta)$ produced overflow as ℓ increased

above values in the stability intervals (see Tables 4.6-4.9). These verify that the stability intervals depend on the various parameters α , β , γ , δ . Using $\theta = 1$, the method $M_2(\theta)$ never produce overflow and always give the qualitatively correct behavior for all $\ell > 0$.

Finally, to study the dynamic of the model (4.1)-(4.4), the three-dimensional distributions of the exact solutions and numerical solutions produced by methods $M_1(\theta = 1)$ and $M_2(\theta = 1)$ are shown in Figures 4.2-4.4. The wave solution of the model produced by method $M_2(\theta = 1)$ at $t = 0, 10, 20, 30$ are shown in Figure 4.5. It is see that the wave solutions are the profile of hyperbolic tangent function which propagate to the right-hand side. As α , β , γ and δ are varies, the wave solutions produced by method $M_2(\theta)$ shall change the amplitude, shape and speed of the wave solutions as shown in Figures 4.6-4.9.

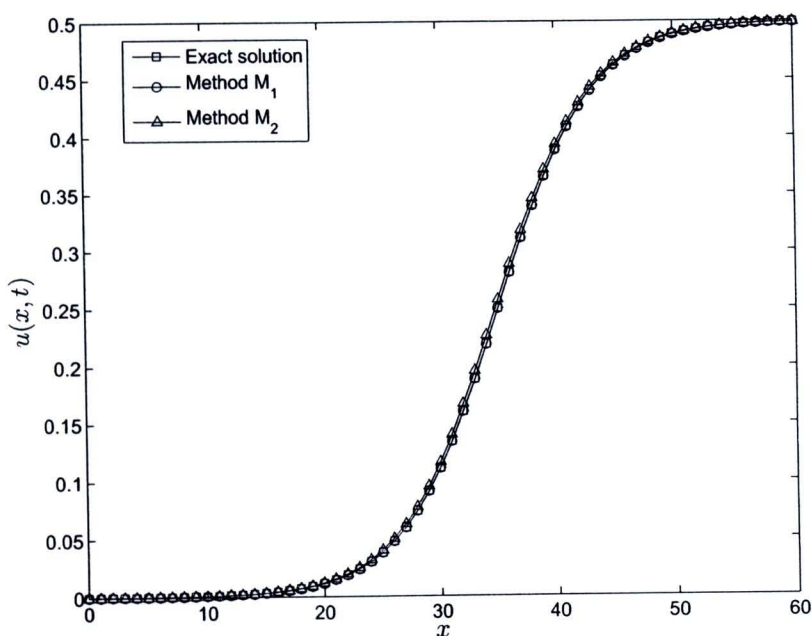


Figure 4.1: The comparison of analytic solution and numerical solution computed by method $M_1(\theta)$ and $M_2(\theta)$ at time $t = 20$ with $\alpha = 1$, $\beta = 1$, $\gamma = 0.5$, $\delta = 1$, $\theta = 1$, $\ell = 0.01$ and $h = 1$

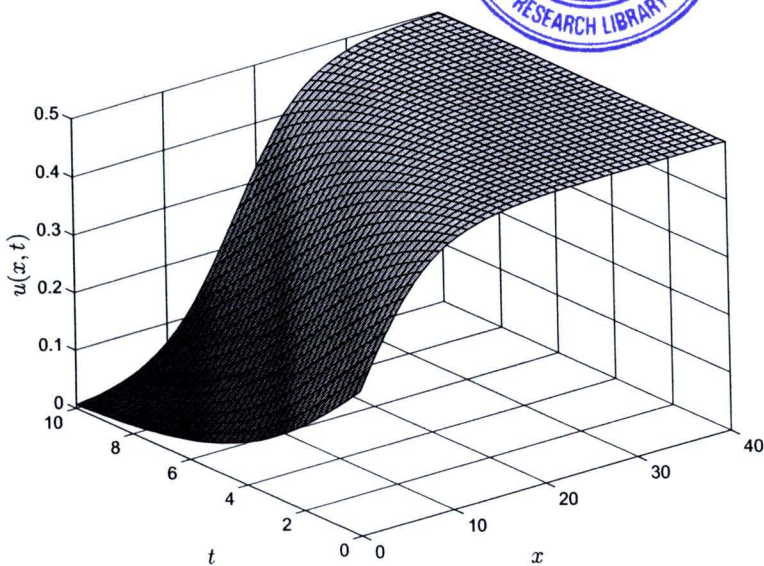


Figure 4.2: The analytic solution of (4.1)-(4.4) with $\alpha = 1$, $\beta = 1$, $\gamma = 0.5$, $\delta = 1$, $\ell = 0.25$ and $h = 1$

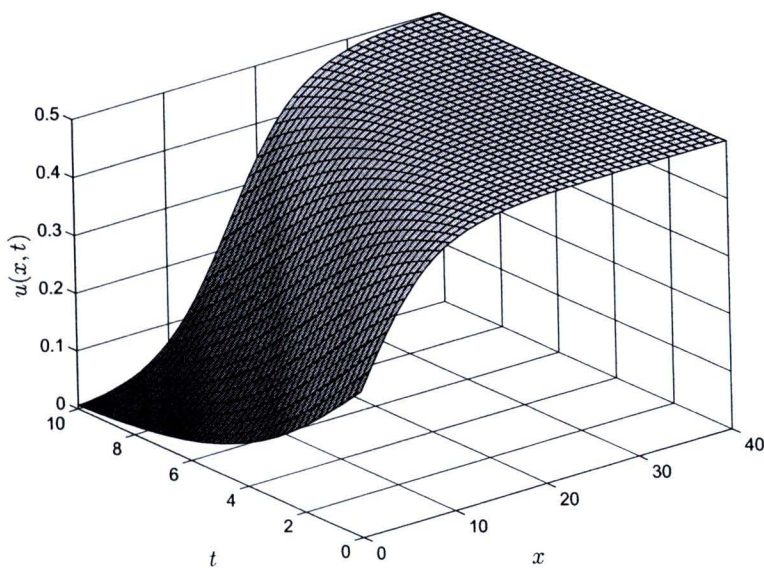


Figure 4.3: The numerical solution of (4.1)-(4.4) using method $M_1(\theta)$ with $\alpha = 1$, $\beta = 1$, $\gamma = 0.5$, $\delta = 1$, $\theta = 1$, $\ell = 0.25$ and $h = 1$

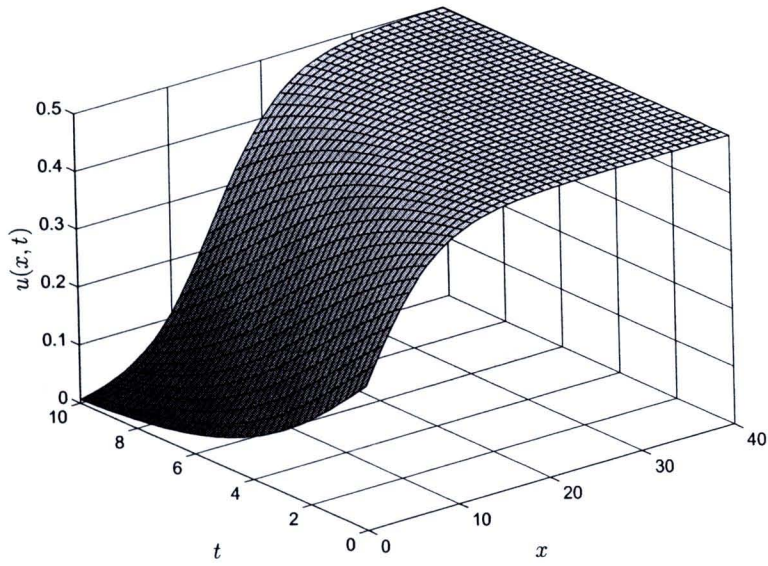


Figure 4.4: The numerical solution of (4.1)-(4.4) using method $M_2(\theta)$ with $\alpha = 1$, $\beta = 1$, $\gamma = 0.5$, $\delta = 1$, $\theta = 1$, $\ell = 0.25$ and $h = 1$

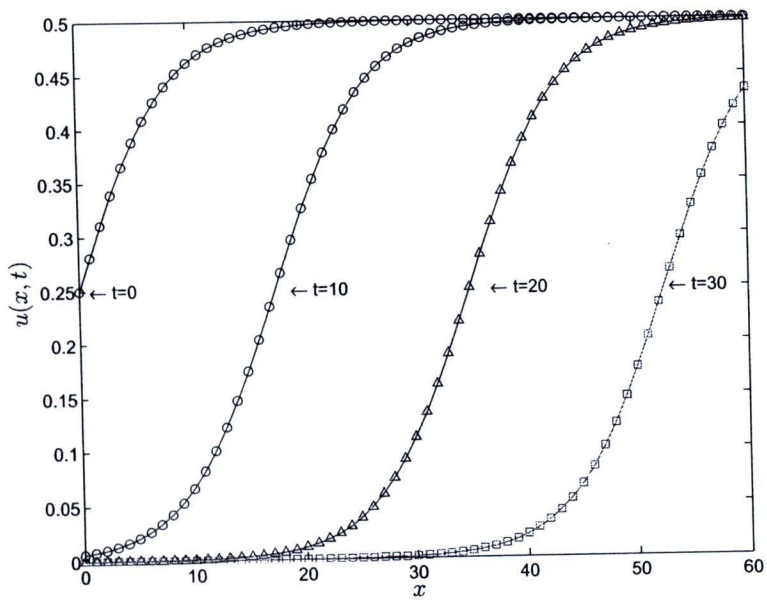


Figure 4.5: The travelling waves of (4.1)-(4.4) at time $t = 0, 10, 20$ and 30 using method $M_2(\theta)$ with $\alpha = 1$, $\beta = 1$, $\gamma = 0.5$, $\delta = 1$, $\ell = 0.01$ and $h = 1$

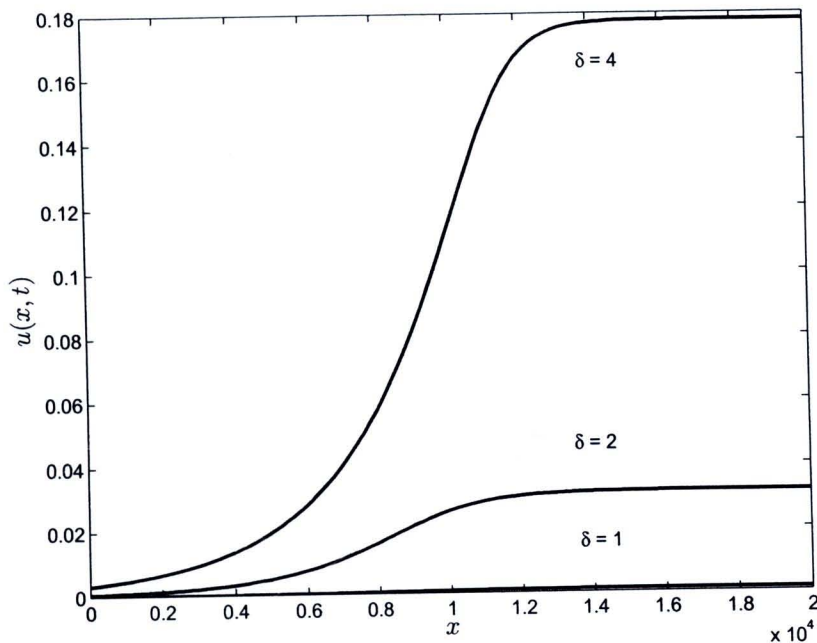


Figure 4.6: The travelling waves of (4.1)-(4.4) at time $t = 4000$ computed by method $M_2(\theta)$ with $\theta = 1$, $\ell = 2$, $h = 200$, $\alpha = 1$, $\beta = 1$ and $\gamma = 0.001$ and vary δ : $\delta = 1$, $\delta = 2$, $\delta = 4$.

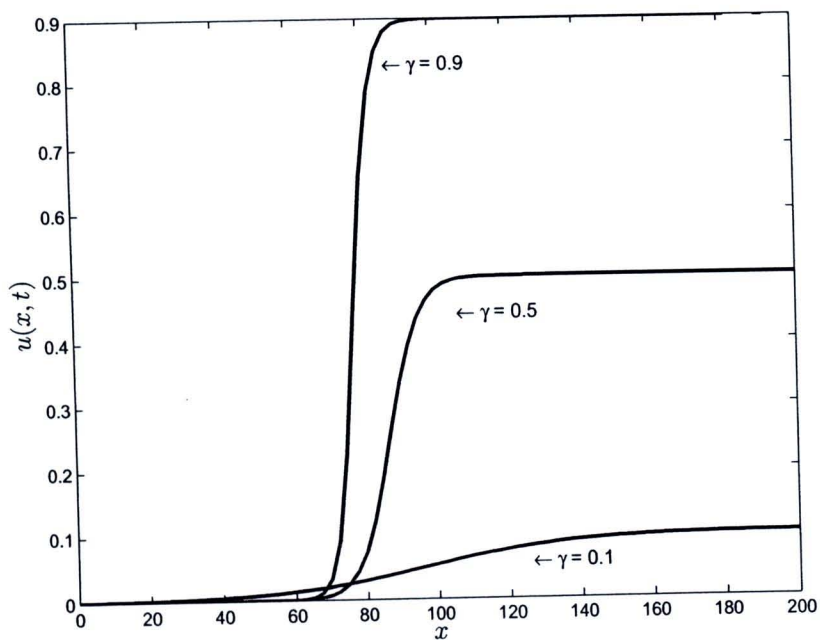


Figure 4.7: The travelling waves of (4.1)-(4.4) at time $t = 200$ computed by method $M_2(\theta)$ with $\theta = 1$, $\ell = 0.25$, $h = 2.5$, $\alpha = 1$, $\beta = 1$ and $\delta = 1$ and vary γ : $\gamma = 0.1$, $\gamma = 0.5$, $\gamma = 0.9$.

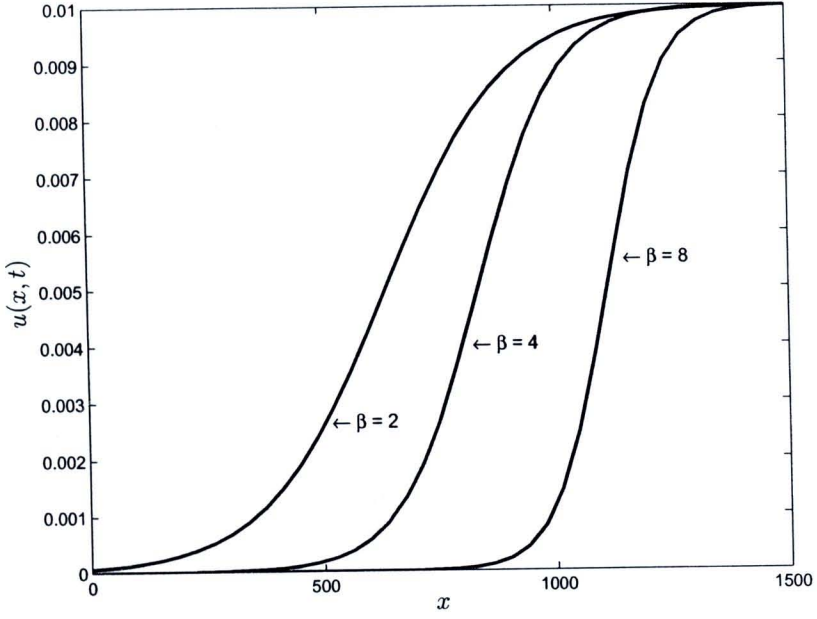


Figure 4.8: The travelling waves of (4.1)-(4.4) at time $t = 250$ computed by method $M_2(\theta)$ with $\theta = 1$, $\ell = 0.125$, $h = 12.5$, $\alpha = 1$, $\gamma = 0.01$ and $\delta = 1$ and vary β : $\beta = 2$, $\beta = 4$, $\beta = 8$.

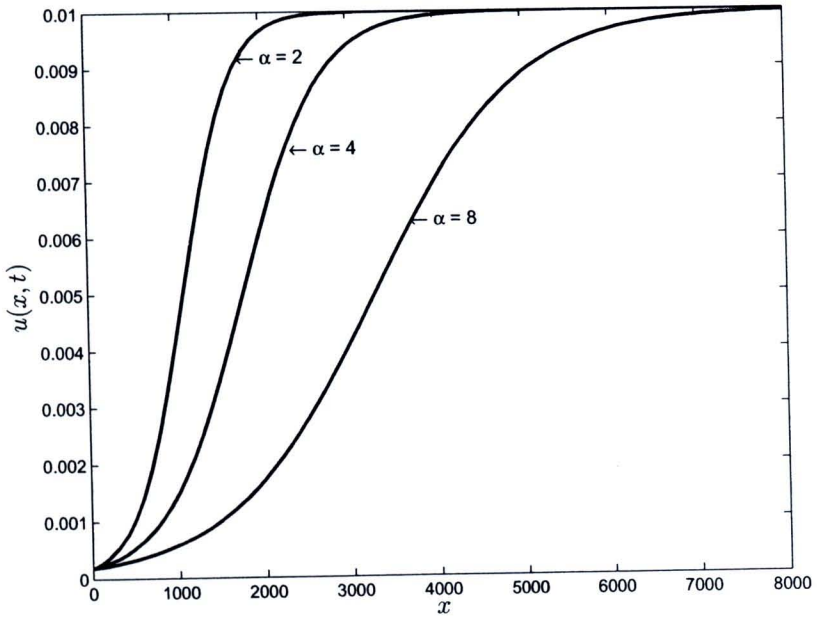


Figure 4.9: The travelling waves of (4.1)-(4.4) at time $t = 400$ computed by method $M_2(\theta)$ with $\theta = 1$, $\ell = 1$, $h = 100$, $\beta = 1$, $\gamma = 0.01$ and $\delta = 1$ and vary α : $\alpha = 2$, $\alpha = 4$, $\alpha = 8$.